ADVANCED MATERIALS INTERFACES
Open Access
www.advmatinterfaces.de

Conductive Gel Phantoms for Training in Electrosurgery

Lorenzo Migliorini, Giacomo Valaperta, Fabio Acocella, Tommaso Santaniello, Nicolò Castelli, Alessandro Perin, Francesco Cavaliere, Maurizio Vertemati, Gian Vincenzo Zuccotti, and Paolo Milani**

Considering the increasing demand for personalized surgical care, as well as current healthcare resources limitations, the use of anatomical accurate 3D physical phantoms is becoming increasingly important for the training of surgeons and the test of surgical instruments. A lack of physical models is nowadays denoted regarding the training in electrosurgery, despite its wide diffusion in medical practice. This work reports an extensive characterization of electrosurgical physical phantoms fabricated with tissue-mimicking ionogels and hydrogels. A careful design of the conductive gels allow the fine tuning of their mechanical and electrical properties, in order to match those of biological tissues. The manufacturing of a novel multi-material skin stratification bench-top pad is reported together with its use for training in both cold and electrical surgery. Furthermore, a feasibility study is reported, showing the use of conductive ionogels for simulating the coagulation of cortical vessels during brain surgery.

1. Introduction

Nowadays, the global healthcare trend is characterized by the increasing demand for personalized surgical services in a context where shrinking economic resources and population ageing require more efficient and targeted approaches to ensure the quality of assistance and its economic sustainability.[1] In addition, current restrictions on working-hours, material resources and economic opportunities, have a significant impact on the quality of resident training, increasing concern about the most effective way to train residents while maintaining patient safety and improving surgical outcomes.[2]

In recent years, there has been growing interest in the use of 3D physical simulation-based models with realistic representations of human anatomical structures and pathologies that allow trainees and surgeons to focus on mastering the individual steps and technical skills required to perform complex procedures in a controlled and risk-free environment.[3] Surgical simulators also provide a more sustainable and versatile solution to current surgical training that exploits cadavers and animal models, which both lack pathological similarity or realism and are becoming less accessible and affordable, having also ethical implications.[4] Physical models can be distinguished between biological, synthetic or hybrid ones.[5] The advantages of synthetic phantoms are mainly represented by easier supplying and longer durability. Also, physical models are often coupled with virtual counterparts, achieving a level of realism that allows surgery students to gain confidence with operating procedures and to better understand the complex anatomical details of the body.[6,7] Low-cost bench-top pads are a typical examples of today's common physical models.[8,9] Surgeons can employ them to learn common practices such as sutures, endoscopic foreign body removal or laparoscopic techniques, to practice skills like hand-eye coordination and manual dexterity, to develop critical psychomotor, technical and judgment skills.[10–12] High-fidelity anatomical phantoms represent a more advanced version of physical models. They aim at

L. Migliorini, G. Valaperta, T. Santaniello, F. Cavaliere, P. Milani
Interdisciplinary Centre for Nanostructured Materials and Interfaces (CIMaINa)
Physics Department
University of Milan
Milan 20133, Italy
E-mail: lorenzo.miglioini@unimi.it; paolo.milani@mi.infn.it

The ORCID identification number(s) for the author(s) of this article can be found under https://doi.org/10.1002/admi.202400246

DOI: 10.1002/admi.202400246

F. Acocella
Department of Veterinary Medicine and Animal Sciences (DIVAS)
University of Milan
Lodi 26900, Italy

N. Castelli, A. Perin
NeuroSim Center and First Division of Neurosurgery
IRCCS Foundation Carlo Besta Neurological Institute
Milan 20133, Italy

M. Vertemati, G. V. Zuccotti
Department of Biomedical and Clinical Sciences "L. Sacco"
University of Milan
Milan 20157, Italy

replicating more complex anatomical situations in the most complete possible way, making use of different advanced materials and techniques.[13] Such models can be employed not only for practitioners training, but also for the evaluation of novel diagnostic and therapeutic procedures, instruments and machineries.[14] Physical models need to meet two main requirements: extremely high anatomical fidelity of native organs and haptic mechanical response. In fact, phantoms need to precisely replicate anatomical shapes, and also possess the mechanical properties able to mimic the surgeon-patient or instrument-patient physical interaction.[15] Therefore, the employed materials and fabrication techniques have to be chosen in order to achieve these requirements which are particularly demanding in the case of soft tissues. Soft materials commonly employed are represented by silicones and hydrogels.[16] Silicones have the advantage of a long-term stability, even if they are usually too elastic and sticky in respect to biological tissues.[17] Hydrogels based on polyvinyl alcohol (PVA), gelatine or agar, usually replicate with good fidelity the haptic properties of water-rich biological tissues, but their storage is more critical since they easily dehydrate.[13,18] The employed soft materials are usually processed in the desired morphology by mean of molding or 3D printing, which allows the manufacturing of anatomically accurate, patient-specific models, characterized by complex shapes and morphologies.[3,18,19]

Considering different surgical techniques that would benefit from the use of phantoms and physical models, electrosurgery is surely one of these. It represents a set of techniques that employ an energy device radiofrequency-based producing electric current that carries to, coagulate, dissect, or carbonize the tissue.[20] An alternating potential difference is applied in a specific area of the body, causing the oscillation of the ions present in the blood. This phenomenon dissipates a huge amount of thermal energy, causing tissues denaturation to dehydration and necrosis, which can either lead to coagulation or cutting. Typically, electrosurgery is performed in two possible configurations: monopolar and bipolar. In the first one the scalpel can be used for both cutting and coagulation; in this setting the energy passes through the body from an active electrode, the tip of the instrument, to a neutral one, generally positioned under the body of the patient. In the bipolar setting the energy passes between the tips of an instrument, usually forceps pinching a small fragment of tissue and the energy doesn't cross the body. The latter configuration is ideal for the coagulation of small structures as blood vessels.[21,22] A lack of physical models is nowadays denoted regarding the training in electrosurgery, despite its wide diffusion in medical practice. The design and the manufacturing of electrosurgical phantoms would require a multi-material approach, able to combine both electrically inert and electro-sensitive materials, whose electrical properties should be similar to those of biological tissues.[23] Very few works can be found on this topic, and they are mainly focused on agar and gelatin hydrogels, possibly combined with biological matter.[24–27] However, the employed materials are characterized by difficult supply, fast dehydration and poor durability, which represent critical aspects for a real implementation in surgical training.

Here we report the fabrication of conductive tissue-mimicking materials, employed for the fabrication of low-fidelity phantoms for practical electrosurgical training. Conductive hydrogels and ionogels are formulated and synthesized, thanks to the combination of different fabrication techniques (like solvent casting and UV photo-polymerization) and precursors (acrylates, polysaccharides, ionic liquids).[28–36] Their mechanical and electrical properties, their durability and their response to electrosurgical techniques have been studied and compared to those of biological tissues. Low-fidelity electrosurgical phantoms are designed, manufactured and tested, addressing two real clinical cases: a multilayered bench-top pad mimicking the skin stratification, and cortical vessels coagulation during brain surgery.

2. Results and Discussion

2.1. Formulation and Synthesis of Hydrogels and Ionogels

Several soft conductive materials have been formulated, synthesized, characterized and tested with electrosurgical techniques. Different formulations of hydrogels and ionogels, with different electrolyte mass content m_{EL} (wt.%) have been explored and modified to reach values of ionic conductivity (0.5 – 5.0 mS cm^{-1}) and mechanical properties (elastic modulus of 10^3 – 10^8 Pa) typical of biological tissues, as well as durability at ambient conditions.[23,37–42] A suitable ionic conductivity represents the most important requirement to achieve, since electrosurgical physical principle is based on the electrical current delivered by the ions inside a patient's tissue. Seven different formulations have been tested, obtained with three different techniques: (i) agar physical hydrogel (AGAR) via sol-gel transition; (ii-vi) three chemical hydrogels (PHA, PHAS, PHAV_E) and two chemical ionogels (PHA-OB and PH-CL) via UV photo-polymerization; (vii) a cellulose-derived physical ionogel (C-CL) via solvent casting. Thin films have been produced for each formulation, as shown in **Figure 1**. (i) Agar is a natural occurring polysaccharide, and AGAR hydrogel is constituted by a physical network of hydrogen bonds amongst the different polymeric chains, formed by a heating-cooling sol-gel transition. Its three-dimensional lattice can retain a high amount of water where NaCl can be dissolved at physiological concentration (0.9 wt.%), providing electrical properties similar to those of biological tissues (electrolyte mass content m_{EL} = 97%).

Cross-linked gels have been synthesized via UV radical photo-polymerization, combining different vinylic species. (ii) 2-hydroxyehtyl methacrylate (HEMA, H) and acrylonitrile (AN, A) have been employed as co-monomers for the production of PHA hydrogel, using poly(ethylene glycole diacrylate) (PEGDMA) as the cross-linker. (iii) A third anionic co-monomer, Na-4-vinylbenzensulfonate (VBS, V), has been used to obtain PHAV hydrogel in order to increase the water uptake, while (iv) PHAV_E has been formulated with ethylene glycole dimethacrylate (EGDMA, E), a cross-linking agent shorter than PEGDA, aiming at reducing the gel elasticity. After the synthesis, these hydrogels have been soaked in aqueous solutions of NaCl 0.9 wt.%, to provide the needed ionic conductivity and reaching electrolyte mass contents m_{EL} of 31.0% (PHA), 83.5% (PHAV) and 78.7% (PHAV_E). The different values are due to the different hydrophilicity and elasticity of the polymeric structures. Photo-polymerization was also employed for the synthesis of two ionogels: (v) PHA-OB (m_{EL} = 63.6%), whose ionic liquid is the synthetic 1-(2-hydroxyethyl)−3-methylimidazolium tetrafluoroborate (OEMIM BF_4, OB), and (vi) PH-CL (m_{EL} = 66.7%) with the

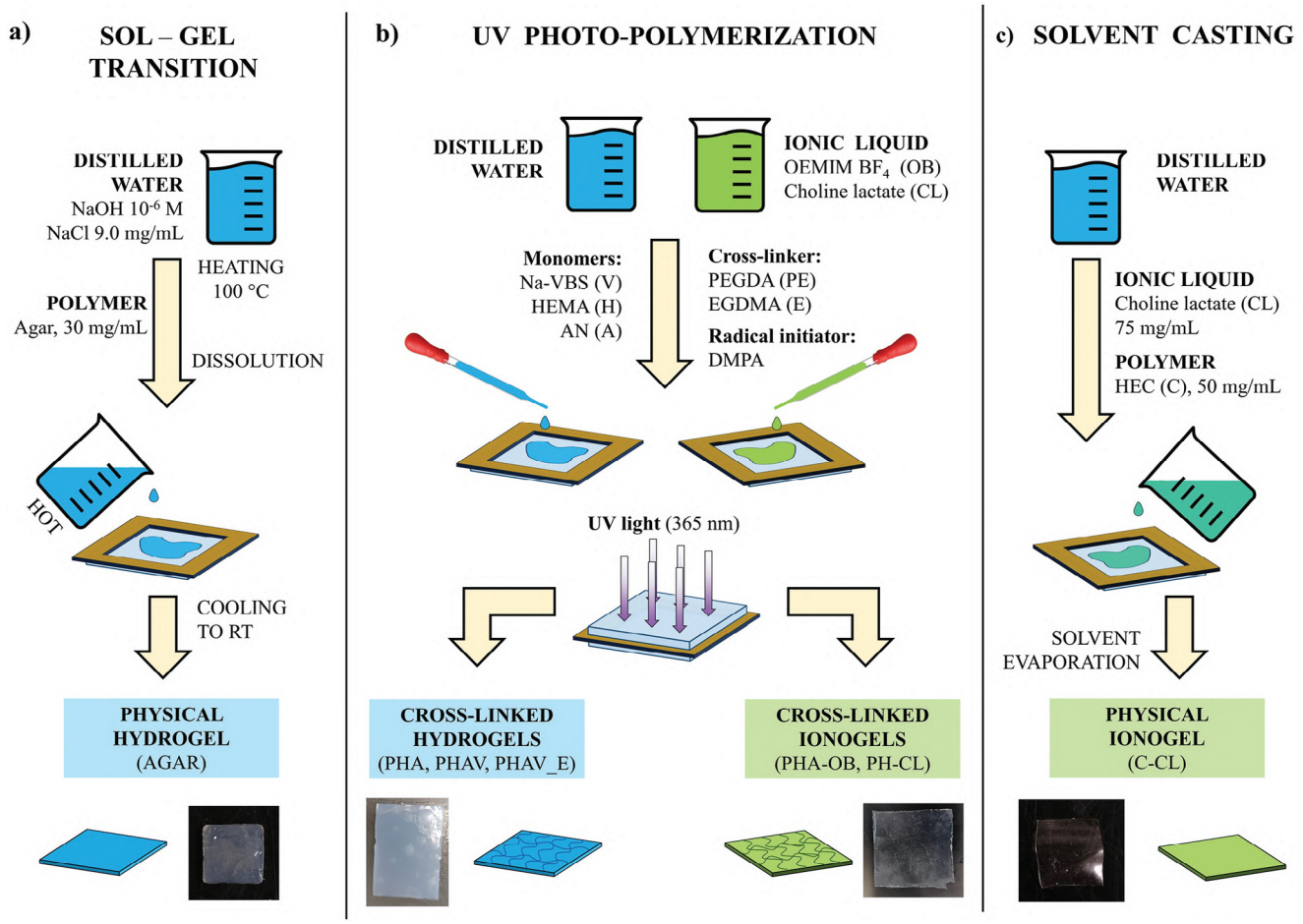

Figure 1. Schematics showing the employed techniques and the procedures to obtain thin films of conductive gels. a) Physical hydrogels of agar have been obtained via sol-gel transition process. b) UV photo-polymerization made it possible to chemically cross-link both hydrogels and ionogels, starting from vinylic monomers. c) physical ionogels based on cellulose have been obtained via aqueous solvent casting.

biodegradable choline lactate (CL) ionic liquid. Last, (vii) C-CL ionogel films have been casted from distilled water, combining two natural-derived substances: 2-hydroxyethyl cellulose (C) and choline lactate (CL).[29] The soft and solid structure is maintained by many physical interactions, such as hydrogen bonds and chain entanglement. In this case, ionic conductivity is provided by the ionic liquid itself, that also absorbs humidity at ambient conditions (m_{EL} = 72.8%).

2.2. Phantom Gels Characterization and Evaluation

The obtained gels (4 hydrogels and 3 ionogels) have been designed to be used as electro-sensitive materials in physical models and phantoms to train electrosurgical techniques. Therefore, they need to mimic the physical properties of human biological tissues, so that a practitioner surgeon can perceive a haptic response while having his hands on them. With this in mind, the mechanical and electrical properties of the different samples have been characterized and compared to those of biological tissues. The material stability and durability over time have been tested as crucial parameters, and their response to electrosurgery has been evaluated with the use of an electric scalpel in a monopolar configuration. The collected information was used to identify which of the various candidates was the most promising for the realization of phantoms for two real clinical cases.

2.2.1. Electrolyte Content, Dehydration and Durability

Figure 2a,b shows the electrolyte mass contents of the obtained samples (m_{EL} wt.%), compared to the average water content of many biological tissues (m_W wt.%), whose average values were taken from literature.[23] AGAR hydrogel possess the highest m_{EL} = 97%, even higher than the typical water content of human tissues, thanks to the high hydrophilicity of its long polymeric chains. PHA hydrogel shows instead the lowest m_{EL} (31%), likely due to the absence of ionic groups in its polymeric structure. In fact, the additional sulfonate anionic group of PHAV hydrogel resulted in a higher m_{EL} = 79%. A slightly lower value (72%) was found for PHAV_E, where the shorter cross-linker reduces the structural hydrogel's stretchability and the consequent amount of water it can absorb. Lastly, all the three ionogels possess electrolyte contents between 64% and 73%, which is the sum of ionic

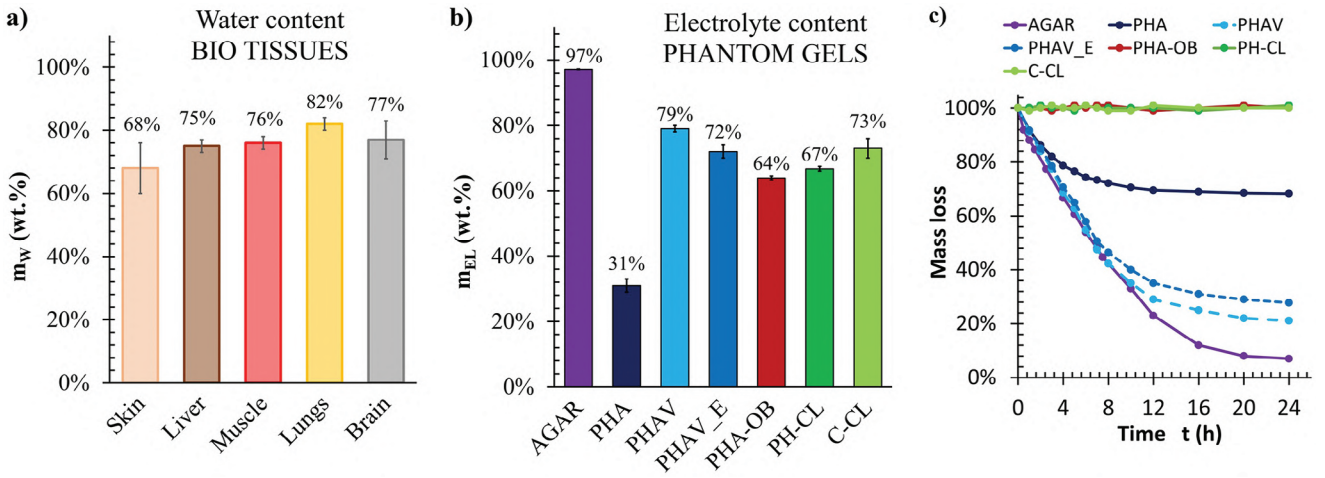

Figure 2. a,b) Histograms showing the average water content of biological tissues and the electrolyte mass content of the reported gel materials.[23] c) Relative mass loss underwent by the different gels, due to dehydration at ambient conditions for 24 hours.

liquid and humidity absorbed from the environment (see Experimental Section). Overall, five out the seven produced gels have electrolyte mass contents comparable to the typical values of many human soft tissues, such as skin, liver, muscles, brain and lungs. The gels durability over time has also been studied, by leaving them at ambient conditions for 24 hours. As can be seen in Figure 2c, all the 4 hydrogels underwent a fast dehydration, as can be expected by considering the aqueous nature of their electrolyte content. The extent of such dehydration resulted to go hand in hand with the electrolyte mass content. In fact, PHA hydrogel with the lowest value of m_{EL} = 31% underwent a mass loss of ca. 30% in 24 hours, while the high electrolyte content AGAR hydrogel lost more than 90% of its original mass. Of course, a huge dehydration also causes a variation in size, as well as in the mechanical and electrical properties, constituting a critical drawback in the durability of phantoms based on hydrogels. Ionic liquids are known for not evaporating at ambient conditions, resulting in all the 3 ionogels to maintain their electrolyte content over time.[43,44] Therefore, ionogels showed to possess a strategic advantage over hydrogels for the realization of tissue-mimicking phantoms for surgical training.

2.2.2. Mechanical Properties

Tissue-mimicking phantoms are expected to possess mechanical properties similar to those of biological tissues. Therefore, all the obtained hydrogels and ionogels have been characterized by mean of linear tensile tests, to identify their Young's (elastic) modulus E and ultimate strain ϵ_{max}. **Figure 3a** reports the obtained plot for each sample. AGAR hydrogel resulted to be the least deformable gel, with a low ultimate strain of 9% and a modulus of ca. 3.6×10^5 Pa. The low strain is also coherent with the extremely high liquid content (m_{EL} = 97%), that weakens the integrity of the gel. Instead, chemically cross-linked hydrogels showed higher strain values, thanks to the reversible folding and unfolding of covalently bound polymeric chains. PHAV and PHAV_E possess the same molar amount of cross-linker, but PEGDA has a higher length and molecular weight than EGDMA, allowing a higher stretching before breaking. This is reflected by the values of ultimate elongation, which is 39% for PHAV and 28% for PHAV_E. Instead, PHA hydrogel is the formulation characterized by the lower hydration level, resulting in a resistant structure with a higher ϵ_{max} = 128%. The Young's Modulus turned out to be quite similar, ca. 1×10^5 Pa, for all the three cross-linked hydrogels. Besides, the produced ionogels possessed a greater variability in mechanical properties. PHA-OB displayed a Young's Modulus $E = 1.8 \times 10^5$ Pa at a strain ϵ_{max} = 49%, while PH-CL showed to be much softer and elastic, with a low $E = 1.4 \times 10^3$ Pa and a high ϵ_{max} = 333%. This discrepancy is likely due to a different interaction between the polymeric matrix and the two distinct ionic liquids: the less polar OB and the more hydrophilic CL. Instead, the typical mechanical strength of cellulose resulted in the tougher C-CL ionogel, with a high Young's Modulus of 1.33×10^6 Pa at ϵ_{max} = 136%. Figure 3b,c reports a comparison between the mechanical properties of biological tissues (averaged from literature)[40–42] and the produced phantom gels. A great variety of values can be found, within which it is possible to identity some nice matchings. The high elastic modulus of the skin (in the order of 10^8 Pa)[42] cannot be matched by any of the produced gels, while its ultimate strain of ca. 54% resulted to be easier to replicate, for example by the PHA-OB ionogel (ϵ_{max} ca. 49%). The Young Modulus of muscular tissues (order of 10^6 Pa)[40] resulted to be suitably matched by the C-CL ionogel, even if the last results way too stretchable. A good match could be found with all the three cross-linked hydrogels, which showed an elastic modulus E very similar to that of liver tissues, in the order of 10^5 Pa.[42] Moreover, PHAV and PHAV_E hydrogels also possess similar elongation at break (ca. 30%), proving to be good candidates for the mimicking of liver tissues. Last, the softer biological tissues of the lungs and the brain possess a Young's modulus of ca. $3 - 4 \times 10^3$ Pa,[41,42,45] which was mostly approached by PH-CL ionogel, even if its value of E remains at least four times higher (1.4×10^4 Pa). The maximum strain values of 50 – 150% for lungs and 20 – 60% for the brain, can be matched by PHA and C-CL gels (ϵ_{max} of 130 – 140%), and by PHAV, PHAV_E and PHA-OB gels (ϵ_{max} of 25 – 50%), respectively. Therefore, the performed characterization showed how the presented pool of

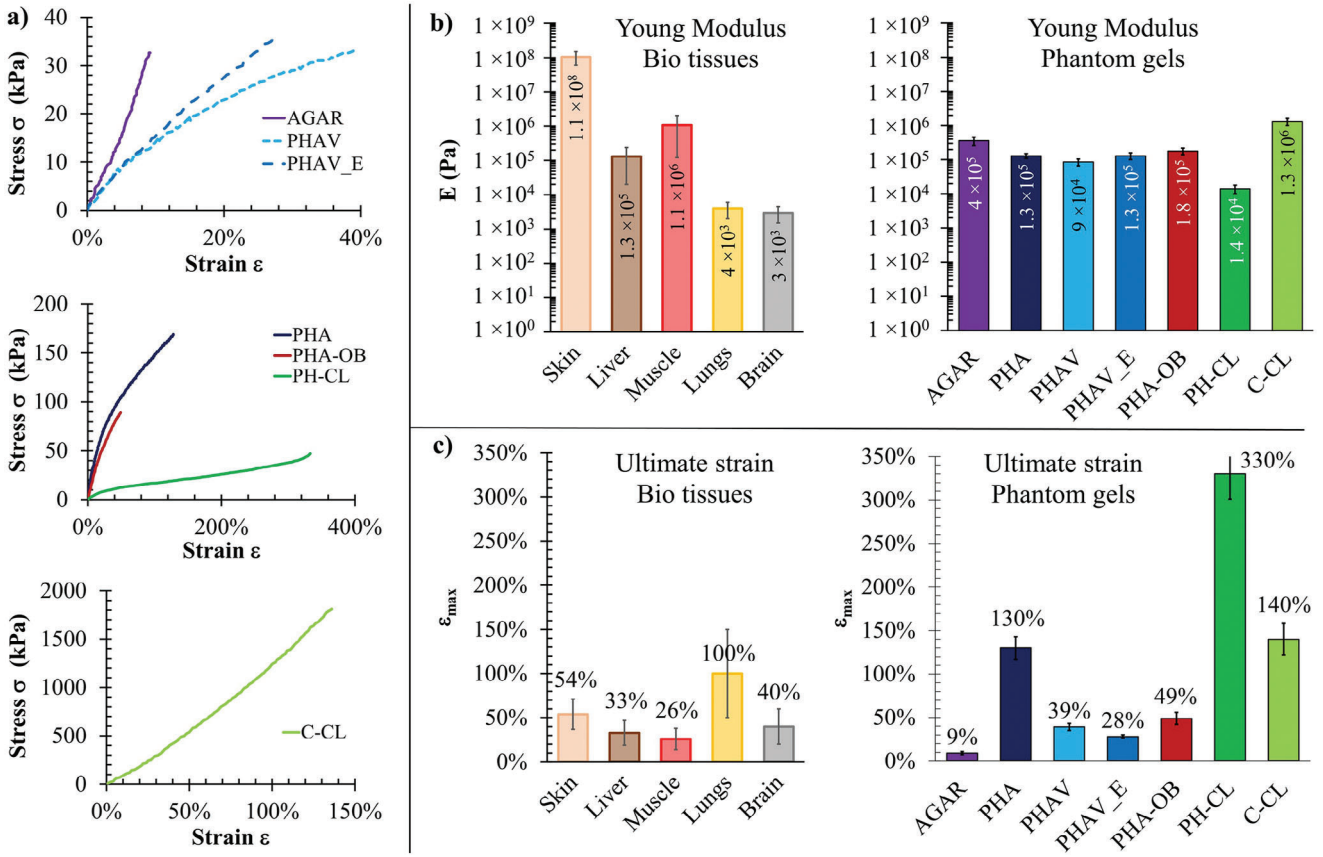

Figure 3. a) Plots reporting the stress-strain curves obtained for the reported gels by means of linear tensile tests. b,c) Young Modulus and ultimate strain values of the reported gels, compared to those of biological tissues (averaged from literature).[40–42,45]

tissue-mimicking gels can replicate the mechanical properties of many biological tissues. Although further studies are needed to perfectly match both the elastic modulus and the ultimate strain, these results demonstrate their suitability for the development of surgical phantoms able to provide a haptic mechanical response.

2.2.3. Conductivity and Electrosurgery Test

The phantom gels need to be responsive to electrosurgical techniques and instrumentation, such as mono and bipolar electric scalpels, and to do so they must possess electrical properties similar to those of biological tissues. Therefore, all the obtained hydrogels and ionogels have been studied by means of electronic impedance spectroscopy (EIS) and **Figure** 4a shows the resulting plot. As can be seen, all the samples possess similar electric behavior, even if of different extent. At high frequencies (10^4–10^6 Hz) the current is mainly delivered by the electrolyte's ionic species, which are Na^+ and Cl^- for the hydrogels, and the ionic liquid's cations and anions for the ionogels. At intermediate frequencies (10^0–10^4 Hz) the current is mainly due to the ionic accumulation in the characteristic double-layer at the gel-electrode interface, while at the lowest frequencies (10^0–10^{-2} Hz) the ionic flow has been saturated in favor of a mainly electronic current inside the gel materials. The high-frequency ionic conductivity σ_{HF} was calculated for each sample as the average value between 10^5 and 10^6 Hz, which is the typical frequency range employed by electrosurgical techniques. Such values are shown in Figure 4b, secondary axis, in comparison with the conductivity of typical biological tissues.[23,37,39] First of all, it can be seen how the conductivity is directly correlated with the electrolyte content (m_{EL} wt.%, primary axis). Besides the employment of three different electrolytes (aqueous solution of NaCl 0.9%, imidazolium-based ionic liquid and choline lactate), it is clear how the high-frequency conductivity directly depends on their mass percentage. This represents a crucial aspect for the design of phantom gels whose conductive properties can be tuned by selecting the correct amount of electrolyte to embed into the polymeric matrix. Also, good matchings can be found by comparing the obtained values with those of biological tissues. In particular, the ionogels with choline lactate ionic liquid (PH-CL and C-CL) possess conductivities in the range of 1.0 – 2.5 mS cm^{-1}, which fits with the 2.2 – 6.5 mS cm^{-1} average range of soft biological tissues. After that, a standard electric scalpel has been employed to "operate " square films of the conductive gels, as if they were thin slices of biological tissues, as it is sketched on the left of Figure 4c. For each tested sample, the instrument passive electrode was placed in contact with a high portion of the gel to guarantee a high contact area, while the tip of the scalpel was employed in two different ways: dragged against the gel's surface to simulate a cutting, or put in contact in a single point to simulate a coagulation. During a real electrosurgery, different current intensities can be employed by the surgeon,

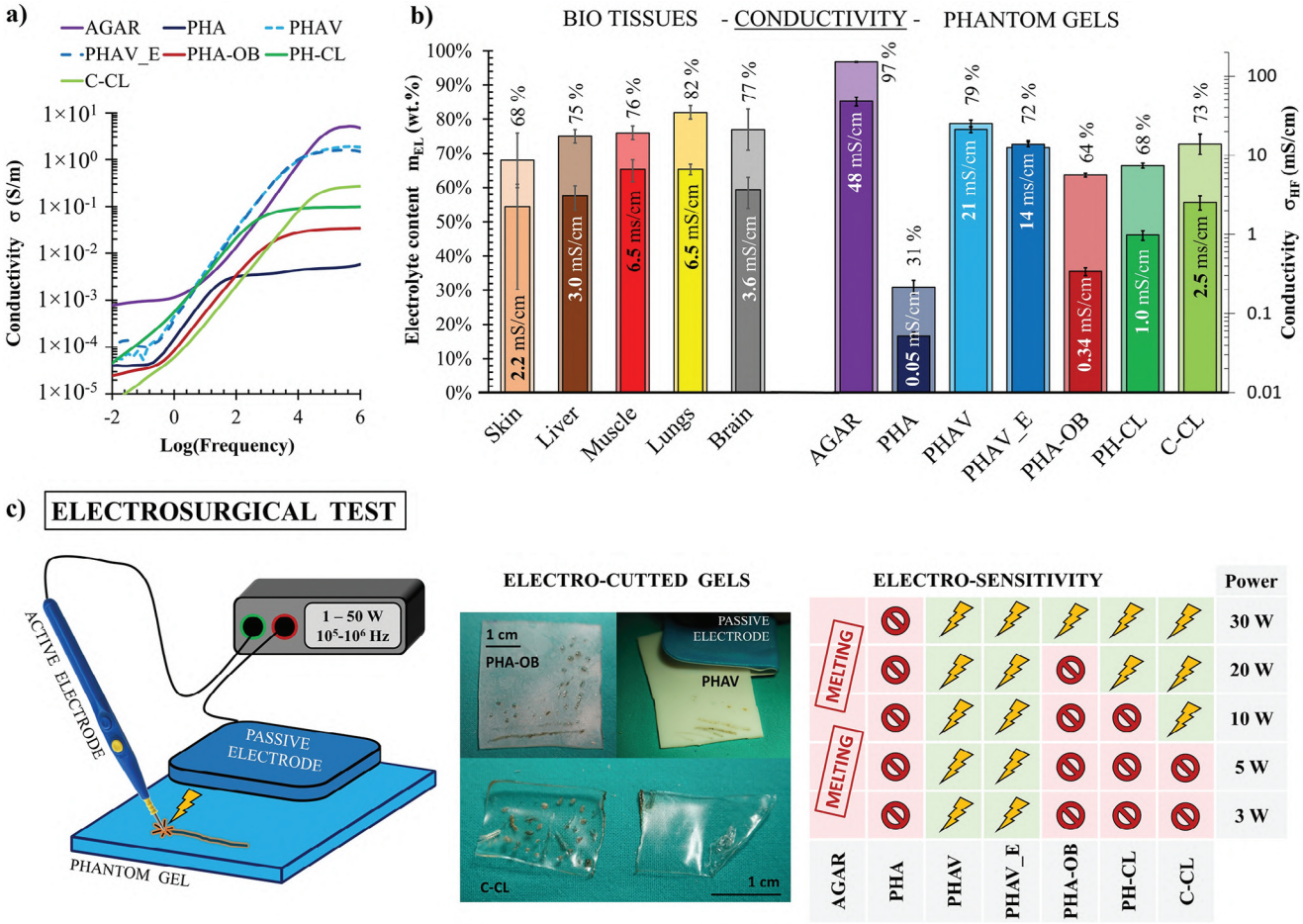

Figure 4. a) Graph reporting the conductivity of the different reported gels, plotted against the applied frequency during electronic impedance spectroscopy measurements. b) Histogram reporting the conductivity (in the foreground, secondary axis) and the electrolyte content (in the background, primary axis) of the reported phantom gels and biological tissues (averaged from literature).[23,37,39] c) The left side of the figure shows a schematics of the experimental setup employed for the electrosurgery tests; shootings of the electro-cut gels are shown in the middle, while on the right side a table is reported, showing the responsiveness of the various gels to different power levels.

according to the tissue type, the precision needed and the damage risk; therefore, different power levels from 3 to 30 W have been tested. The majority of the gels have been successfully "operated", with a couple of exceptions. The least conductive PHA hydrogel (σ_{HF} = 0.05 mS cm^{-1}) resulted to be inert to the electric scalpel tips, clearly because of its poor ionic conduction, way lower than biological matter. Instead, despite the high conductivity (σ_{HF} = 48 mS cm^{-1}) of AGAR hydrogel, the contact with the scalpel caused melting rather than burning of the gel surface. This phenomenon was already reported by Amiri et al.[27] and it can be explained by considering the synthesis technique of AGAR hydrogel. In fact, unlike the other gels, obtained via solvent casting or UV photo-polymerization, AGAR hydrogel has been formed by a heating-cooling sol-gel transition, where the heat causes the dissolution of the polymeric chains and the subsequent cooling induces the gelation of the solution. Therefore, it's logical to consider that the Joule heating caused by the device induces a phase transition to the AGAR hydrogel, bringing the polymeric chains back to solution and causing a superficial melting rather than a burning.

Besides PHA and AGAR hydrogel, five out the seven reported phantom gels have been successfully tested, with the tip leaving behind a burned trace on the gel's surface. Some photographs are shown in the middle of Figure 4c, where it is possible to notice both longer (cut) and shorter (coagulated) burned traces. Different power levels have been tested and the samples electro-sensitivity is shown in the table on the right of Figure 4c. Such sensitivity resulted to be coherent with the previously measured ionic conductivities. More in detail, PHAV and PHAV_E hydrogel, whose σ_{HF} was of 14 – 21 mS cm^{-1}, showed to be sensitive to the electric scalpel down to power levels of 3 W. All the ionogels, with lower conductivities between 0.3 and 2.5 mS cm^{-1}, needed a power of at least 10 W to reach a current density high enough to induce burning. Two videos are reported in Supporting Information, showing the effect of the electric scalpel on PH-CL ionogel, at power levels of 20 and 30 W. These results are particularly relevant since it is the first reported case where ionogels have been tested with electrosurgical techniques as tissue-mimicking phantom materials. Also, it has been demonstrated how it is possible to tune the electro-sensitivity of hydrogels and ionogels by

controlling their electrolyte content and the consequent ionic conductivity.

2.2.4. Material Comparison and Evaluation

Seven different formulations of conductive gels have been synthesized and studied. Their mechanical and electrical properties have been characterized and compared to those of biological tissues, showing good similarities and proving their tunability through a smart materials design process. Their durability, as well as their actual responsiveness to an electric device have been tested as well. Then, all the gathered information has been employed to carry out an evaluation process, aimed at identifying which of them represents the best candidate, or the best candidates, for the realization of tissue-mimicking phantom prototypes inspired by real clinical cases. AGAR and PHA hydrogels have been discarded: the first underwent melting rather than burning during the tests, while the low conductivity of the second made it inert to electrosurgical techniques. The other two hydrogels, PHAV and PHAV_E, appear to be much more promising. Their water content (72–79%) is the same of soft biological tissues, their ultimate elongation (28–39%) is similar to that of muscles, liver and brain, and their high ionic conductivity (14–21 mS cm^{-1}) made it possible to employ the device even at low power levels (down to 3 W). Unfortunately, they present a huge drawback which is typical of hydrogels: fast dehydration at ambient conditions. In fact, both PHAV and PHAV_E underwent a mass loss of ca. 30% in only 4 hours, which became more than 50% after 3 additional hours. The electrolyte's loss also changes the shape as well as the mechanical and electrical properties of the gels, which limits dramatically the available time window for a surgeon practitioner to work on it, and it also generates issues concerning their storage between production and employment. On the other hand, the electrolyte content and the physical properties of ionogels remain stable over time, as previously shown. This represents a great advantage of this class of gel materials over their hydro- counterpart. PHA-OB ionogel displayed a maximum elongation (49%) similar to that of brain and skin tissues, however its ionic conductivity of 0.34 mS cm^{-1} resulted to be quite low, making this material sensitive to the energy only with a high power of 30 W. Therefore, the higher conductivity of PH-CL and C-CL (1.0 and 2.5 mS cm^{-1}, respectively) makes them better candidates for the development of electrosurgical phantoms, also considering the non-toxic nature of choline lactate in respect with the imidazolium based ionic liquid of PHA-OB. The Modulus of Young of PH-CL (1.4×10^4 Pa) is few times higher than lungs and brain tissues, while that of C-CL (1.3×10^6 Pa) is more similar to muscular tissues. Both of them demonstrated to be suitable tissue-mimicking soft materials with adequate responsiveness to electrosurgical techniques. However, C-CL solvent casting technique is more suited for the production of thin films rather than three-dimensional structures. Also, the absence of covalent bonds between the polymeric chains causes the dissolution of C-CL ionogel after contact with water, making this material ineffective in those situations where a surgeon needs to spray physiological aqueous solution. On the contrary, UV photopolymerization is a technique that allows the manufacturing of chemically cross-linked 3D gels that do not dissolve in case of contact with a solvent. Therefore, PH-CL ionogel was identified as the most promising amongst the reported tissue-mimicking materials, and it was the one selected for the realization of electrosurgical phantom prototypes, inspired by real clinical cases.

2.3. Electrosurgical Phantom Prototypes

2.3.1. Skin Stratification Bench-Top Pad for Electrosurgery

Electrosurgery, understood as the use of radiofrequency devices to dissect the anatomical stratigraphy of which biological tissues, including entire organs, are composed is a common practice in surgery, which optimizes visualization of structures of interest, creates hemostasis, and speeds up operative time. Despite being a widespread practice, it is not present in any artificial simulation devices used in surgical education. We chose as an initial approach to test the efficacy of our electrosensitive material on the simplest device used in surgical simulation: a typical multilayer surgical pad extensively employed in recent years for the training of dozens of surgery students and residents. In our case, part of the layers, the connective tissue, are substituted by the conductive ionogel. In this setting the learner could experience either cold and electrosurgical dissection techniques, mimicking a real biological situation. As it sketched in **Figure** 5a, different biological tissues are stacked in layers in the human body, each of them characterized by different properties and functions. During surgery, the surgeon must work his way through these layers of tissue in order to reach the patient's affected areas.

As can be seen in the Figure, all the different tissue layers have been replicated with synthetic materials. Muscle, muscle band, adipose tissue (fat) and skin are usually torn apart with a traditional bisturi, therefore no electrical sensitivity is needed and insulant silicone-based elastomers have been employed as tissue-mimicking materials. On the contrary, the two layers of connective tissue are usually torn apart with the use of an electric scalpel, therefore they were simulated with the electro-sensitive PH-CL. The ionogel was also employed to integrate in the structure a couple of ionic bridges (Figure 5b), in order to put the electro-sensitive layers in electrical contact with the base of the pad, and in turn with the instrumentation's collector plate. The so obtained phantom was tested for the simulation of a real operation, where a surgeon was able to alternatively apply both cold and electrosurgical techniques. Figure 5c shows some shooting of the process, while four videos can be found in the Supporting Information, showing the operations sequentially conducted by the surgeon: resection of the "skin" layer with a cold scalpel; burning of the upper "connective tissue" layer with an electric scalpel; tearing apart of the "fat" layer via cold surgery; burning of the lower "connective tissue" layer with the electric scalpel. After 30 days, the PH-CL electro-sensitive layer maintained its structural integrity and conductivity, showing a durability that could never be achieved with phantoms based on hydrogels rather than ionogels.

2.3.2. Cortical Vessels Coagulation

Brain surgery was the second targeted clinal case: a feasibility study was performed regarding cortical vessels coagulation. In

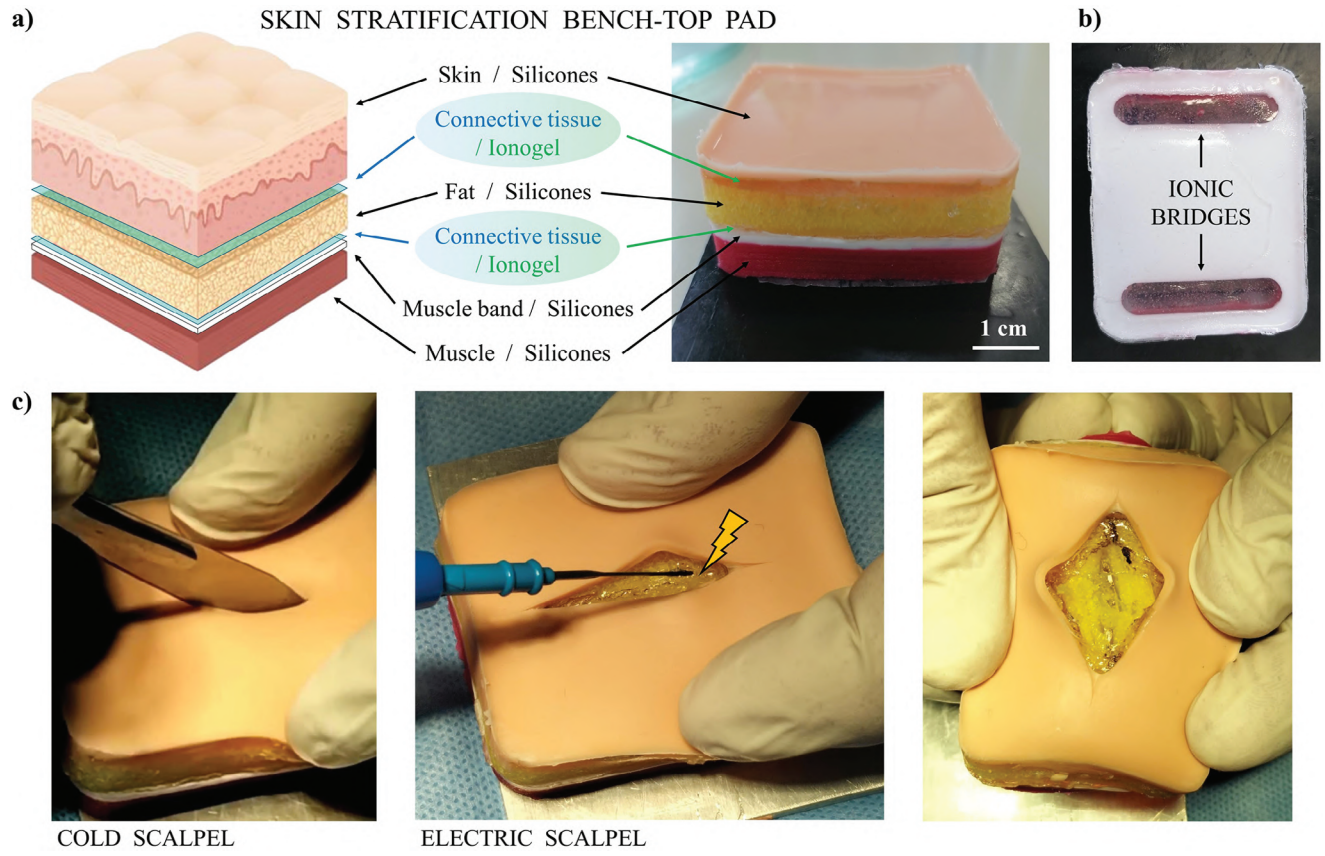

Figure 5. a) A schematic of the different layers that constitute the skin stratification, correlated with the tissue-mimicking bench-top pad developed in this work, whose layers are constituted by silicone elastomers and the PH-CL ionogel. b) Top-view of the muscle – muscle band – connective tissue layers, highlighting the presence of the two ionic bridges needed to put the electro-sensitive layers in electrical contact with the base of the pad. c) Shooting of the surgery simulation on the bench-top pad: starting from the left, it can be seen the surgeon tearing apart the "skin" with a cold scalpel, and the "connective tissue" with an electrical one, showing in the end, the resected tissues.

fact, to operate the inner part of the brain, surgeons need to make their way through a dense network of blood vessels of different dimensions. To prevent cerebral hemorrhage, the vessels need to be cauterized before being torn apart, and electrosurgery is the technique usually employed for this purpose. Unlike the monopolar electric scalpel, cortical vessel coagulation is carried out with bipolar forceps, with the current passing in the region between the two pincers. A typical operation is shown in **Figure** 6a, while Figure 6b shows a cortical vessel network. The production of physical models and phantoms would be extremely beneficial for the training in a such delicate procedure. To achieve this goal, electro-sensitive artificial vessels need to be developed and embedded in more complex brain phantoms. In this work, a feasibility study is reported. PH-CL ionogel has been employed to produce artificial cortical vessels, by mean of a manual embedded 3D-printing process.[46] More in detail, the ionogel pre-polymeric solution was manually injected into a silicon oil bath. The injection rate was controlled in order to obtain self-standing and continuous liquid traces, which maintain their shapes thanks to a balance between polar-apolar and viscous interactions with the surrounding silicon oil. After the deposition of the traces, the bath was placed under a UV light to initiate the photo-polymerization, obtaining irregular worm-like ionogel solid structures (Figure 6c).

The so obtained PH-CL artificial vessels have been tested with surgical bipolar forceps by a brain surgeon. As it is shown in Figure 6d, the high current density inside the gel induced a local sizzle, whose optical, haptic and acoustic perception resembled a lot the coagulation process of a real cortical vessel. A video of this test can be found in the Supporting Information. The obtained results proved how PH-CL ionogel can be employed for the free-form fabrication of artificial cortical vessels, suitable for the simulation of electrosurgical coagulations with bipolar forceps. However, the reported results must be considered preliminary, since the control on the embedded 3D-printing is still manual and the obtained artificial vessels are yet to be incorporated in a full brain phantom.

3. Conclusion

A comparative study has been conducted amongst different conductive gel materials, combining different substances and fabrication techniques. Soft hydrogels and ionogels have been synthesized and characterized, comparing their electrical and mechanical properties with those of biological tissues. The use of

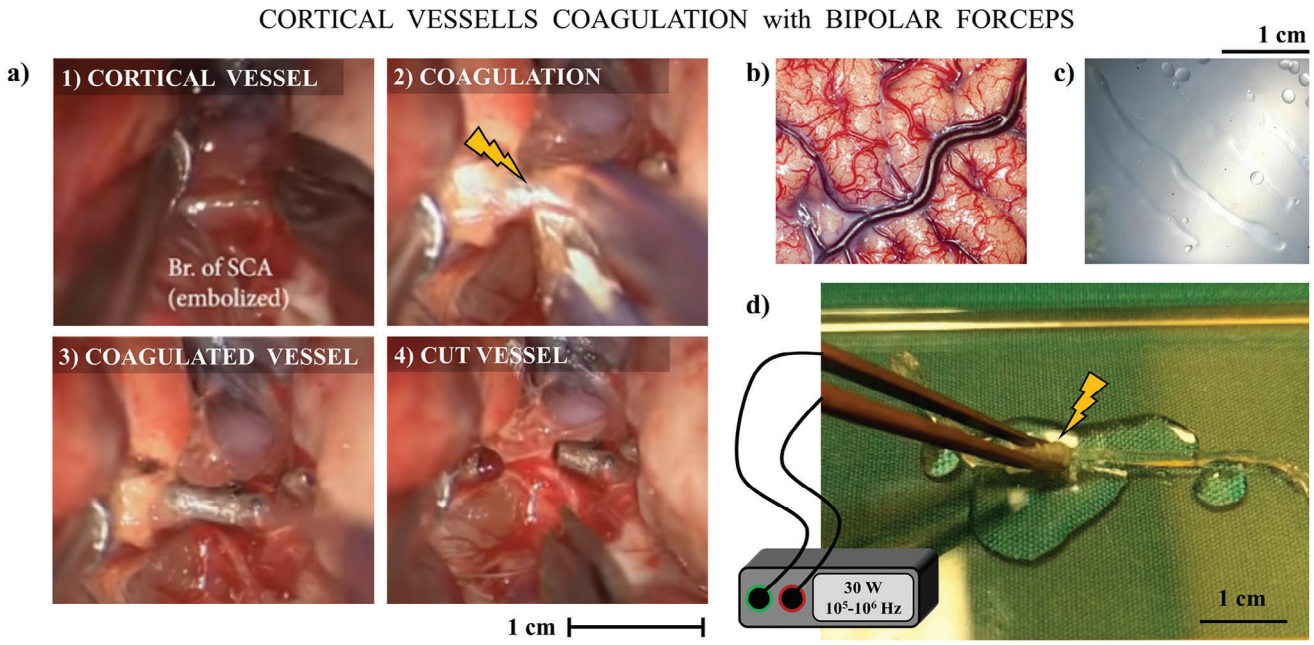

Figure 6. a) Screenshot sequence showing the sequential steps of a specific operation in brain surgery: 1) the identification of a cortical vessel to be resected, 2) vessel coagulation with a bipolar scalpel (forceps), 3) the coagulated vessel, within the blood flow is blocked and 4) the cutting of the coagulated vessel, preventing hemorrhage. Reproduced with permission.[47] Copyright 2019, Journal of Neurosurgery Publishing Group. b) Picture showing a network of cortical vessels. c) Self-standing and continuous liquid traces of PH-CL pre-polymeric solution injected inside a silicon oil bath. d) Tissue-mimicking blood vessels based on PH-CL used by a brain surgeon to simulate a cortical vessel coagulation procedure with a real bipolar forceps.

stable and durable ionogels was demonstrated to overcome the de-hydration issues typical of hydrogel-based phantoms. The most promising ionogel was obtained by the combination of a natural-derived ionic liquid (choline lactate) with a photo-polymerizable acrylic polymer (PHEMA). Then, the realization of phantoms for two real clinical cases have been targeted. First, a multilayered bench-top pad has been manufactured with the integration of both electro-sensitive and inert materials, mimicking a patient's skin stratification, where a surgeon was able to alternatively apply both cold and electrical surgery. The second targeted clinical case was represented by brain surgery: conductive gel has been employed to produce artificial cortical vessels, by means of a manual embedded 3D-printing process. A feasibility study was performed, where a surgeon was able to employ bipolar forceps to simulate the coagulation process of a real cortical vessel (even if a full brain phantom was not developed in this work). All considered, the reported results can constitute a solid and promising background for the further development and diffusion of tissue-mimicking phantoms for surgical and electrosurgical training.

4. Experimental Section

Materials: Agar powder, 2-hydroxyethyl cellulose (M_w = 380 g/mol) (HEC, C), 2,2-dimethoxy-2-phenylacetophenone (DMPA), 2-hydroxyethyl methacrylate (HEMA, H), Na-4-vynilbenzene sulfonate (Na-4-VBS, V), ethylene glycole dimethacrylate (EGDMA), poly(ethylene glycole diacrylate) (M_w = 575 g/mol) (PEGDA), dimethyl sulfoxide (DMSO), sodium chloride (NaCl), have been purchased from Sigma Aldrich. Acrylonitrile (AN, A) has been purchased from Fluka. The ionic liquids 1-(2-hydroxyethyl)−3-methylimidazolium tetrafluoroborate (HO-EMIM BF_4, OB) and choline lactate (CL) haven been purchased from Iolitec. Sodium hydroxide aqueous solution (1 mol L^{-1}) has been purchased from Riedel-de Haen.

Conductive Gel Synthesis: Agar hydrogels (AGAR) have been obtained via sol-gel transition. The 1 M aqueous solution of NaOH has been diluted 1:10^6, to obtain 100 mL of NaOH 10^{-6} M (pH = 8), where NaCl (0.9 g) has been dissolved under magnetic stirring. The solution has been heated at ca. 100 °C and agar (3 g) has been added. After 10′, the solution has been poured into Teflon or aluminum open molds, where the solution quickly went through gelation. The obtained 1 and 3 mm-thick AGAR hydrogel films have been stored at ca. 4 °C. The chemically cross-linked hydrogels have been obtained via UV radical photo-polymerization. The initiator solution has been prepared by dissolving DMPA powder in DMSO at a concentration of 50 mg mL^{-1}. PHA hydrogel's pre-polymeric solution has been prepared my mixing HEMA and AN (molar ratio 6:4) in distilled water, with a total monomer concentration of 7.7 M, together with PEGDA (4.0×10^{-2} M). Na-4-VBS was added in the pre-polymeric solutions of PHAV and PHAV_E hydrogels (VBS:HEMA:AN molar ratio of 1:6.5:2.5), and EGDMA was added in place of PEGDMA for the PHAV_E formulation. Each solution has been magnetically stirred for 30′ at room temperature, the DMPA initiator solution has been added and, after 10′ of additional stirring, the solution has been poured inside a silicon frame ($90 \times 90 \times 1$ cm^3) clamped by a couple of glass slides. The mold has been subjected to UV irradiation (wavelength of 365 nm) for 40′. Afterward, the mold has been opened, the hydrogels removed and stored in a 9 g/L NaCl aqueous solution. The cross-linked ionogels have been obtained with the same procedure, but the monomers, cross-linker and radical initiator have been dissolved in the ionic liquid rather than water, with a monomer concentration of 1.0 g mL^{-1}. PHA-OB has been obtained with a HEMA: AN molar ratio of 4:6, dissolved in HO-EMIM BF_4, ionic liquid, PH-CL with HEMA as the only monomer dissolved in choline lactate. Last, thin films of physical ionogel C-CL have been obtained via solvent casting. An aqueous solution has been obtained by dissolving the polymer HEC (50 mg mL^{-1}) and the ionic liquid CL (75 mg ml^{-1}), then it has been deposited in a

silicon framework placed on a glass slide. The solvent evaporation led to the formation of 0.2 mm-thick ionogel films.

Electrosurgical Phantom Prototypes: The bench-top pad has been assembled by the staking of silicone layers that simulate human skin stratification: "muscle" (6 mm), "muscle band" (1 mm), "adipose tissue" (6 mm) and "skin" (2 mm). Each layer has been formed by specific recipes protected by industrial secret and owned by the Italian company Huvant – Medical Simulation Platform, a spin-off of the University of Milan. The so-described bench-top pads have been extensively employed in recent years, for the training of dozens of surgery students and residents. Two layers of "connective tissue" have been obtained with the in situ photo-polymerization of 1 mm-thick conductive PH-CL. Each layer below the "skin" has been molded with a couple of transversal holes (35×8 mm^2, distance of 34 mm from each other), filled with PH-CL ionic bridges able to electrically connect the upper and the lower part of the pad. The final pad had dimensions of $60 \times 45 \times 17$ mm^3. Each layer of the pad has been in situ polymerized on top of the underlaying layer, granting robust silicone-silicone and ionogel-ionogel adhesion. Ionogel-silicone adhesion resulted to be lower and it represents an element to improve. Also, PH-CL ionogel has been employed to produce artificial cortical vessels, by means of a manual embedded 3D-printing process. A few milliliters of the pre-polymeric solution have been withdrawn with a syringe, whose needle had an inner diameter of ca. 1 mm. The same syringe has been employed to manually inject the solution into a silicon oil bath with silica particles (5.0 wt.%). The injection rate was manually controlled in order to obtain self-standing and continuous liquid traces, with a diameter of 1–2 mm. After the deposition of each trace, the bath was placed under a UV light for 5 minutes to initiate the photo-polymerization, obtaining irregular worm-like ionogel solid structures. Then, all the deposited traces have been subjected to UV light for other 40 minutes, in order to complete their polymerization, prior to their extraction from the silicone bath.

Electrolyte Mass Content and Durability Tests: The electrolyte mass content m_{EL} (wt. %) has been defined as the ratio between the mass of the liquid conductive phase, and the total mass of each gel. m_{EL} of AGAR hydrogel has been calculated starting from its formulation, by comparing the mass of NaCl aqueous solution and the polymeric mass, that remain unaltered by the sol-gel process. Instead, PHA, PHAV and PHAV_E hydrogels absorbed the electrolyte after soaking in the 9 g L^{-1} NaCl aqueous solution. Therefore, m_{EL} was calculated comparing the hydrated mass of the hydrogels with their dry mass, obtained after a complete drying of 72 hours in ambient conditions. Concerning PHA-OB, PH-CL and C-CL ionogels, the ionic liquid's mass percentage was calculated starting from their formulation; also, humidity absorption at ambient conditions has been considered. Small specimens of each sample have been subject to durability tests in ambient condition, by regularly measuring their mass loss (due to dehydration) for 24 hours.

Mechanical and Electrical Characterization: Linear tensile tests have been conducted to study the mechanical properties of the obtained conductive gels. Specimen in the typical dogbone shape have been employed for this purpose, with a central region characterized by length, width and thickness of 20, 5 and 3 mm, respectively. An exception was represented by C-CL ionogels, whose thickness was of 1 mm, because solvent casting technique was not suited for the production of thick films. A representative picture of dogbone specimens was reported in the Supporting Information. The strain ϵ has been calculated as the ratio between the traction distance and the original length, the stress σ as the ratio between the measured force and the specimen transversal section. Usually, the Youngs Modulus E was calculated as the ratio between σ and ϵ in the linear region of a stress-strain curve. However, in this work, E has been obtained by considering each stress–strain curve in its entirety, by calculating the ratio between the maximum values of σ and ϵ, reached before breaking. While less accurate, this choice allowed an easier comparison between different formulations of conductive gels and biological tissues. Electrochemical impedance spectroscopy (EIS) has been performed with a Reference 600 Gamry potentiostat, with the superimposition of a sinusoidal potential of 5 mV over a DC = 0 V. Frequencies from 10^{-2} to 10^6 Hz have been explored. $1 \times 1 \times 0.1$ cm^3 samples have been tested, employing copper tape (non-adhesive side) for the connection with the instrument. For each sample, σ_{HF} has been calculated as the average impedance in the frequency range of 10^5 – 10^6 Hz, normalized by the geometry.

Electrosurgery Tests: The electrosurgical device was composed of a ForceTriad Energy Platform (Medtronic) as energy generator, an Electrosurgical Pencils with Edge Coated Electrodes as active electrode and a Valleylab PolyHesive Corded Patient Return Electrodes as passive electrode. Three samples for each formulation have been tested. Each sample has been tested with power levels from 3 to 30 Watt. To close the electrical circuit, the passive electrode was wrapped around one of the edges of the samples, or placed below the tested bench-top pad. In the cortical vessels' coagulation test, a similar device was employed and operated at 30 W, with bipolar forceps working as both the active and the passive electrode.

Statistical Analyses: For each conductive gel formulation, three different samples have been subjected to mechanical and electrical tests. The reported values of the Young's Modulus (E), the maximum strain (ϵ_{max}) and the high-frequency conductivity (σ_{HF}) were referred to the samples that provided intermediate values compared to the other two. The associated standard deviation S was represented by the error bars. Instrumental error propagation has also been conducted, resulting to be lower than S in any case and, therefore, neglected. The electrolyte mass content m_{EL} of PHA, PHAV and PHAV_E hydrogels has been obtained similarly, by comparing the hydrated and dehydrated masses of three different samples for each formulation. The intermediate values were reported, with the associated standard deviation S. m_{EL} of AGAR hydrogel has been theoretically calculated by considering the masses and the volumes employed for the synthesis process. The associated error comes from instrumental error propagation. Concerning PHA-OB, PH-CL and HEC-CL ionogels, the electrolyte mass content was the sum of the ionic liquid and the water uptake from the environment. Therefore, error propagation has been conducted, by combining instrumental errors (associated to the employed amount of ionic liquid) and standard deviations (associated to humidity absorption by three different samples for each formulation). A table can be found in Supporting Information, providing the values reported in the graphs, with their associated errors.

Supporting Information

Supporting Information is available from the Wiley Online Library or from the author.

Acknowledgements

Project within the MUSA – Multilayered Urban Sustainability Action – project, funded by the European Union – NextGenerationEU, under the National Recovery and Resilience Plan (NRRP) Mission 4 Component 2 Investment Line 1.5: Strenghtening of research structures and creation of R&D "innovation ecosystems", set up of "territorial leaders" in R&D.

Conflict of Interest

The authors declare no conflict of interest.

Data Availability Statement

The data that support the findings of this study are available from the corresponding author upon reasonable request.

Keywords

brain surgery, conductive gels, electrosurgery, physical phantoms, surgical training, tissue-mimicking materials

Received: March 21, 2024
Revised: June 17, 2024
Published online:

[1] M. Cristea, G. G. Noja, P. Stefea, A. L. Sala, *Int. J. Environ. Res. Public Health* **2020**, *17*, 1439.
[2] M. M. Hutter, K. C. Kellogg, C. M. Ferguson, W. M. Abbott, A. L. Warshaw, *Ann. Surg.* **2006**, *243*, 864.
[3] M. Higgins, S. Leung, N. Radacsi, *Ann. 3D Print. Med.* **2022**, *6*, 100057.
[4] S. V. Kotsis, K. C. Chung, *Plast. Reconstr. Surg.* **2013**, *131*, 1194.
[5] I. Badash, K. Burtt, C. A. Solorzano, J. N. Carey, *Ann. Transl. Med.* **2016**, *4*, 453.
[6] R. M. Viglialoro, S. Condino, G. Turini, M. Carbone, V. Ferrari, M. Gesi, *Appl. Sci.* **2021**, *11*, 2338.
[7] S. K. Sarker, B. Patel, *Int. J. Clin. Pract.* **2007**, *61*, 2120.
[8] D. Sharma, V. Agrawal, J. Bajaj, P. Agarwal, *J. Surg. Simul.* **2020**, *7*, 33.
[9] T. P. Williams, C. L. Snyder, K. J. Hancock, N. J. Iglesias, C. Sommerhalder, S. C. DeLao, A. C. Chacin, A. Perez, *J. Surg. Res.* **2020**, *256*, 618.
[10] M. Kailavasan, C. Berridge, G. Kandaswamy, B. Rai, *World J. Surg.* **2020**, *44*, 1431.
[11] K. R. Kavanagh, V. Cote, Y. Tsui, S. Kudernatsch, D. R. Peterson, T. A. Valdez, *Laryngoscope* **2017**, *127*, E132.
[12] A. G. Gallagher, E. M. Ritter, H. Champion, G. Higgins, M. P. Fried, G. Moses, C. D. Smith, R. M. Satava, *Ann. Surg.* **2005**, *241*, 364.
[13] E. Choi, F. Adams, S. Palagi, A. Gengenbacher, D. Schlager, P. F. Müller, C. Gratzke, A. Miernik, P. Fischer, T. Qiu, *Ann. Biomed. Eng.* **2020**, *48*, 437.
[14] Z. Zhao, Y. Ma, A. Mushtaq, V. Radhakrishnan, Y. Hu, H. Ren, W. Song, Z. T. H. Tse, *Proc. Inst Mech. Eng. Part H J. Eng. Med.* **2023**, *237*, 3.
[15] S. Maglio, C. Park, S. Tognarelli, A. Menciassi, E. T. Roche, *IEEE Trans. Med. Robot. Bionics* **2021**, *3*, 349.
[16] C. K. McGarry, L. J. Grattan, A. M. Ivory, F. Leek, G. P. Liney, Y. Liu, P. Miloro, R. Rai, A. P. Robinson, A. J. Shih, B. Zeqiri, C. H. Clark, *Phys. Med. Biol.* **2020**, *65*, 1439.
[17] S. Hatamikia, L. Jaksa, G. Kronreif, W. Birkfellner, J. Kettenbach, M. Buschmann, A. Lorenz, *Z. Med. Phys.* **2023**.
[18] C. Richardson, S. Bernard, V. A. Dinh, *J. Ultrasound Med.* **2015**, *34*, 1479.
[19] G. Mazzoleni, T. Santaniello, F. Pezzotta, F. Acocella, F. Cavaliere, N. Castelli, A. Perin, In *The High-risk Surgical Patient*, Cham: Springer International Publishing, **2023**, pp. 621–638.
[20] I. Alkatout, T. Schollmeyer, N. A. Hawaldar, N. Sharma, L. Mettler, *J. Soc. Laparoendosc. Surg.* **2012**, *16*, 130.
[21] K. Gallagher, B. Dhinsa, J. Miles, *Surgery* **2011**, *29*, 70.
[22] K. R. Bulsara, S. Sukhla, S. M. Nimjee, *Neurosurg. Rev.* **2006**, *29*, 93.
[23] T. J. C. Faes, H. A. Van Der Meij, J. C. De Munck, R. M. Heethaar, *Physiol. Meas.* **1999**, *20*, R1.
[24] M. A. Kandadai, J. L. Raymond, G. J. Shaw, *Mater. Sci. Eng. C* **2012**, *32*, 2664.
[25] R. K. Chen, A. J. Shih, *Phys. Med. Biol.* **2013**, *58*, 5511.
[26] B. Eigl, C. Haslebacher, P. C. Müller, A. Andreou, B. Gloor, M. Peterhans, *IEEE Open J. Eng. Med. Biol.* **2020**, *1*, 166.
[27] S. A. Amiri, P. Van Berckel, M. Lai, J. Dankelman, B. H. W. Hendriks, *Biomed. Opt. Express* **2022**, *13*, 2616.
[28] M. Piazzoni, E. Piccoli, L. Migliorini, E. Milana, F. Iberite, L. Vannozzi, L. Ricotti, I. Gerges, P. Milani, C. Marano, C. Lenardi, T. Santaniello, *Soft Robot.* **2021**, *9*, 224.
[29] L. Migliorini, C. Piazzoni, K. Põhako-Esko, M. D. I. Girolamo, A. Vitaloni, F. Borghi, T. Santaniello, A. Aabloo, P. Milani, *Adv. Funct. Mater.* **2021**, *31*, 2102180.
[30] E. Milana, T. Santaniello, P. Azzini, L. Migliorini, P. Milani, *Appl. Nano* **2020**, *1*, 59.
[31] L. Migliorini, T. Santaniello, F. Borghi, P. Saettone, M. C. Franchini, G. Generali, P. Milani, *Nanomaterials* **2020**, *10*, 2062.
[32] L. Migliorini, T. Santaniello, S. Rondinini, P. Saettone, M. Comes Franchini, C. Lenardi, P. Milani, *Sensors Actuators, B Chem* **2019**, *286*, 230.
[33] S. M. Villa, V. M. Mazzola, T. Santaniello, E. Locatelli, M. Maturi, L. Migliorini, I. Monaco, C. Lenardi, M. Comes Franchini, P. Milani, *ACS Macro Lett.* **2019**, *8*, 414.
[34] T. Santaniello, L. Migliorini, F. Borghi, Y. Yan, S. Rondinini, C. Lenardi, P. Milani, *Smart Mater. Struct.* **2018**, *27*, 065004.
[35] T. Santaniello, L. Migliorini, E. Locatelli, I. Monaco, Y. Yan, C. Lenardi, M. C. Franchini, P. Milani, *Smart Mater. Struct.* **2017**, *26*, 085030.
[36] L. Migliorini, T. Santaniello, Y. Yan, C. Lenardi, P. Milani, *Sensors Actuators, B Chem* **2016**, *228*, 758.
[37] H. McCann, G. Pisano, L. Beltrachini, in *Variation in Reported Human Head Tissue Electrical Conductivity Values*, Springer, US, **2019**.
[38] H. Neeb, V. Ermer, T. Stocker, N. J. Shah, *Neuroimage* **2008**, *42*, 1094.
[39] R. Pethig, D. B. Kell, *Phys. Med. Biol.* **1987**, *32*, 933.
[40] J. Zwirner, B. Ondruschka, M. Scholze, N. Hammer, *J. Biomech.* **2020**, *106*, 109829.
[41] S. R. Polio, A. N. Kundu, C. E. Dougan, N. P. Birch, D. E. Aurian-Blajeni, J. D. Schiffman, A. J. Crosby, S. R. Peyton, *PLoS One* **2018**, *13*, 0204765.
[42] G. Singh, A. Chanda, *Biomed. Mater.* **2021**, *16*062004,.
[43] J. L. Bideau, L. Viau, A. Vioux, *Chem. Soc. Rev.* **2011**, *40*, 907.
[44] E. Andrzejewska, A. Marcinkowska, A. Zgrzeba, *Polymers* **2017**, *62*, 344.
[45] M. Lauria, B. Stiehl, A. Santhanam, D. O'Connell, L. Naumann, M. McNitt-Gray, A. Raldow, J. Goldin, I. Barjaktarevic, D. A. Low, *Front. Med.* **2023**, *10*, 1151867.
[46] J. Zhao, N. He, *J. Mater. Chem. B* **2020**, *8*, 10474.
[47] S. Kiyofuji, H. J. Cloft, C. L. W. Driscoll, M. J. Link, *Neurosurg. Focus* **2019**, *1*, 1.

